Biophysical Journal, Volume *116*

Supplemental Information

Engineered Passive Potassium Conductance in the KR2 Sodium Pump

Arend Vogt, Arita Silapetere, Christiane Grimm, Florian Heiser, Maximiliano Ancina Möller, and Peter Hegemann

Supplementary Figure 1

A

abbreviation	organism	protein ID	type (habitat)	literature (cited in the main text)
KR2	*Dokdonia eikasta* (basonym: *Krokinobacter eikastus*)	N0DKS8	flavobacterium (seawater)	Yoon et al. 2012 Inoue et al. 2013
NdR2 (NQRh)	*Nonlabens dokdonensis* (basonym: *Donghaeana dokdonensis)*	L7W3L9	flavobacterium (seawater)	Yi et al. 2012 Kwon et al. 2013
NMR2	*Nonlabens marinus*	W8VZ79	flavobacterium (seawater)	Yoshizawa et al. 2014
YIK11	*Nonlabens sp.YIK11*	X2G242	flavobacterium (seawater)	Kwon et al. 2016
GLR	*Gillisia limnaea*	H2BW50	flavobacterium (antarctic lake)	Balashov et al. 2014
IAR	*Indibacter alkaliphilus*	S2D3K4	(non-flavo) bacterium (halo alkaline lake)	Li et al. 2015
TrNaR1	*Truepera radiovictrix*	D7CSE2	(non-flavo) bacterium (hot alkaline spring)	Ivanova et al. 2011
TrNaR2		D7CW88		

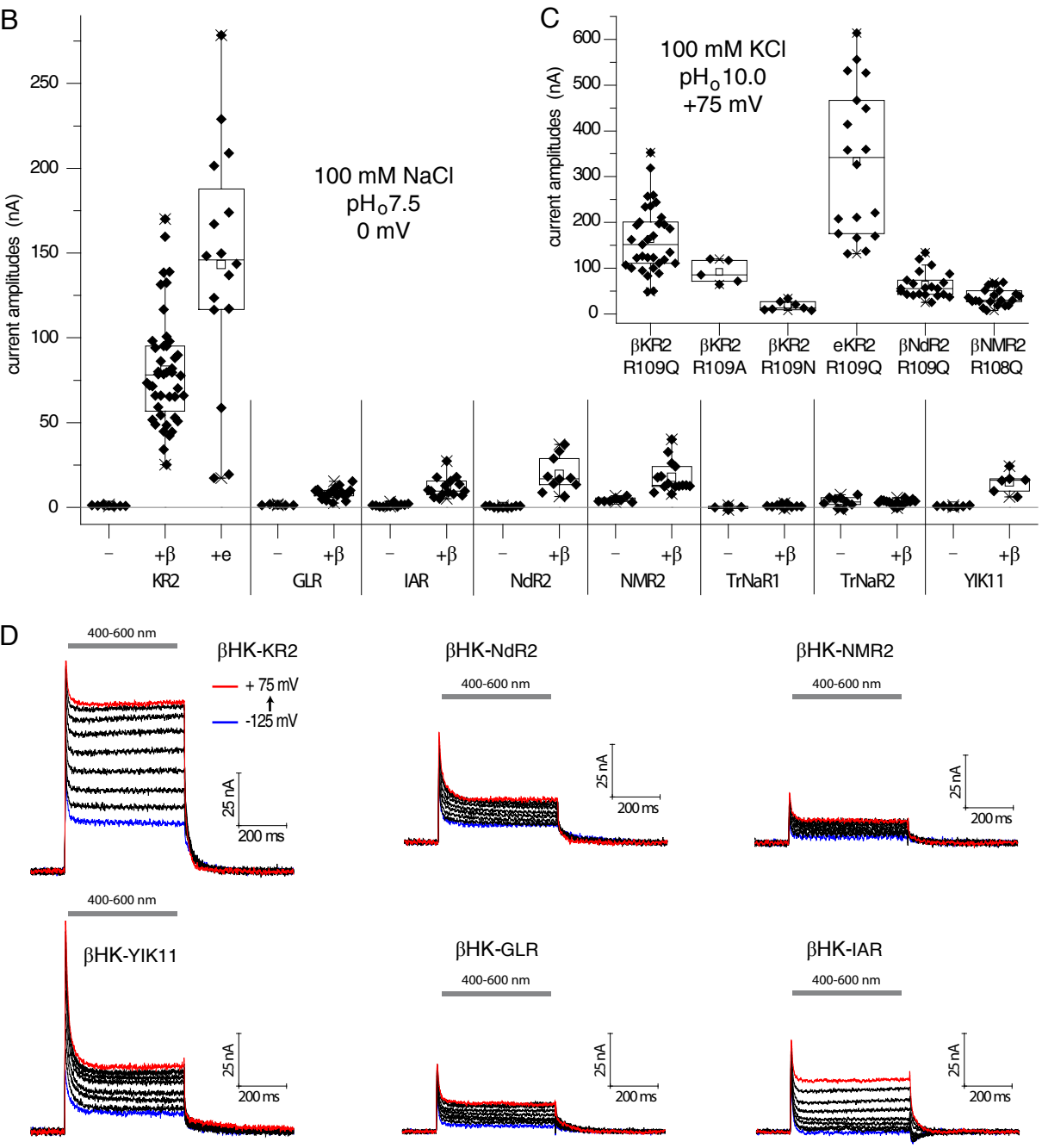

Supplementary Figure 1: Comparison of light-driven Na+ pumps from different organisms in oocytes. (*A*) List of NaRs tested in this study, with their origin and protein ID; references are provided in the main article. (*B-C*) Comparison of absolute stationary photocurrent amplitudes, shown as box-chart diagrams. Detectable photocurrents were only observed after addition of the "βHK"-targeting sequence (the eKR2 targeting design was only tested for KR2). (*C*) Stationary photocurrent amplitudes of the various R109X mutants are shown. In addition to KR2, only NdR2$_{\beta HK}$ and NMR2$_{\beta HK}$ provided sufficient photocurrents for testing the effect of the R109Q mutation (R108 in NMR2). (*D*) Photocurrent traces of various NaRs (all with "βHK") in buffer containing 100 mM NaCl, pH$_o$ 7.5. The IAR rhodopsin was remarkable in that produced showed negative peak-shaped photocurrents at negative holding potentials.

Supplementary Figure 2:

Multiple sequence alinment of NaRs and proton pumps

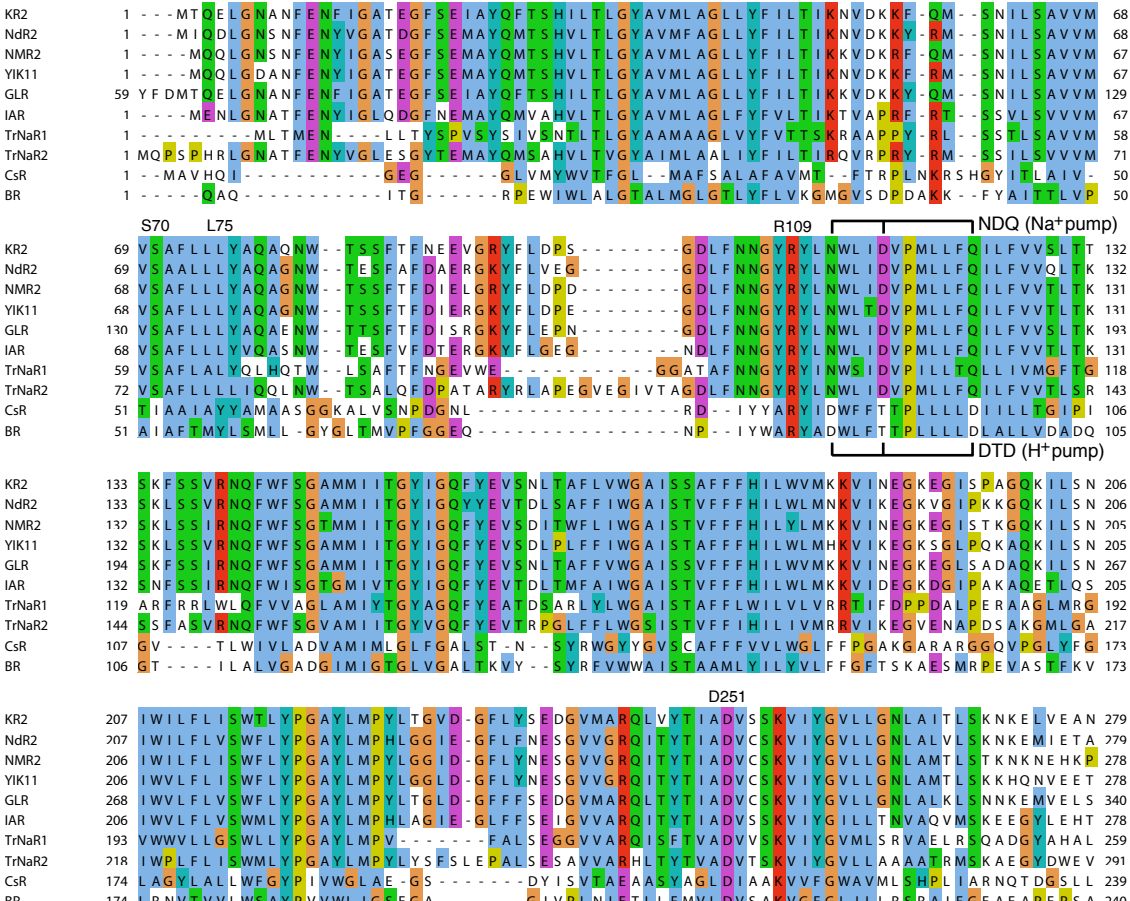

Supplementary Figure 3:

Nucleotide sequence of all tested KR2-constructs

KR2 (oocytes):

ATGACTCAGGAGCTGGGGAACGCTAATTTTGAGAACTTCATTGGAGCCACCGAGGGGTTTTCAGAGATCGCCTATCAGTTTACATCACACATTCTGACTCTGGGATATGCAGTCATGCTGGCCGGCCTGCTGTA
CTTTATCCTGACCATTAAGAACGTGGACAAGAAATTCCAGATGAGTAATATCCTGAGCGCCGTGGTCATGGTGAGCGCCTTCCTGCTGCTGTATGCCCAGGCTCAGAACTGGACTAGCTCCTTTACCTTCAATG
AGGAAGTGGGCCGGTACTTTCTGGACCCAAGTGGCGATCTGTTCAACAATGGGTACAGATATCTGAACTGGCTGATTGATGTGCCCATGCTGCTGTTTCAGATCCTGTTCGTGGTCAGCCTGACCACATCCAAA
TTCTCTAGTGTGAGGAACCAGTTTTGGTTCTCAGGCGCTATGATGATCATTACCGGCTATATTGGGCAGTTTTACGAGGTCAGCAATCTGACAGCATTCCTGGTGTGGGGGGCTATTTCAAGCGCATTCTTTTTC
CATATCCTGTGGGTCATGAAGAAAGTCATCAACGAGGGAAAGGAAGGCATTTCTCCCGCCGGACAGAAAATCCTGAGTAATATCTGGATTCTGTTTCTGATCTCCTGGACACTGTACCCCGGGGCTTATCTGAT
GCCTTACCTGACTGGGGTGGACGGATTCCTGTATTCTGAAGATGGAGTCATGGCACGGCAGCTGGTGTATACAATTGCCGACGTGTCCTCTAAGGTCATCTACGGGGTGCTGCTGGGCAATCTGGCAATTACC
CTGTCAAAAAACAAGGAACTGGTGGAGGCAAATAGCCCGCGGTGA

βHK-KR2 (oocytes):

ATGGCAGCCCTGCAGGAGAAGAAGTCATGCAGCCAGCGCATGGCCGAATTCCGGCAATACTGTTGGAACCCGGACACTGGGCAGATGCTGGGCCGCACCCCAGCCCGGTGGGTGTGGATCAGCCTGTACTA
TGCAGCTTTCTACGTGGTCATGACTGGGCTCTTTGCCTTGTGCATCTATGTGCTGATGCAGACCATTGATCCCTACACCCCCGACTACCAGGACCAGTTAAAGTCACCGGGGGGTAACCTTGAGACCGGATGTGT
ATGGGGAAAGAGGGCTGCAGATTTCCTACAACATCTCTGAAAACAGCTCTACTCAGGAGCTGGGGAACGCTAATTTTGAGAACTTCATTGGAGCCACCGAGGGGTTTTCAGAGATCGCCTATCAGTTTACATC
ACACATTCTGACTCTGGGATATGCAGTCATGCTGGCCGGCCTGCTGTACTTTATCCTGACCATTAAGAACGTGGACAAGAAATTCCAGATGAGTAATATCCTGAGCGCCGTGGTCATGGTGAGCGCCTTCCTGC
TGCTGTATGCCCAGGCTCAGAACTGGACTAGCTCCTTTACCTTCAATGAGGAAGTGGGCCGGTACTTTCTGGACCCAAGTGGCGATCTGTTCAACAATGGGTACAGATATCTGAACTGGCTGATTGATGTGCCC
ATGCTGCTGTTTCAGATCCTGTTCGTGGTCAGCCTGACCACATCCAAATTCTCTAGTGTGAGGAACCAGTTTTGGTTCTCAGGCGCTATGATGATCATTACCGGCTATATTGGGCAGTTTTACGAGGTCAGCAAT
CTGACAGCATTCCTGGTGTGGGGGGCTATTTCAAGCGCATTCTTTTTCCATATCCTGTGGGTCATGAAGAAAGTCATCAACGAGGGAAAGGAAGGCATTTCTCCCGCCGGACAGAAAATCCTGAGTAATATCT
GGATTCTGTTTCTGATCTCCTGGACACTGTACCCCGGGGCTTATCTGATGCCTTACCTGACTGGGGTGGACGGATTCCTGTATTCTGAAGATGGAGTCATGGCACGGCAGCTGGTGTATACAATTGCCGACGTG
TCCTCTAAGGTCATCTACGGGGTGCTGCTGGGCAATCTGGCAATTACCCTGTCAAAAAACAAGGAACTGGTGGAGGCAAATAGCCCGCGGTGA

eKR2 = C2C1-KR2-TS-eYFP-ER (oocytes):

ATGGACTATGGGGGAGCACTGTCCGCCGTCGGGCTGTTTCAGACTTCCTACACCCTGGAGAACAACGGGAGCGTCATTTGCATTCCTAACAATGGCCAGTGCTTCTGTCTGGCCTGGCTGAAGAGCAACGGGA
CCCAGGAACTGGGCAATGCCAACTTTGAGAATTTCATCGGCGCCACCGAGGGCTTTAGCGAGATCGCCTATCAGTTCACCTCCCACATCCTGACACTGGGCTATGCCGTGATGCTGGCCGGCCTGCTGTACTTT
ATCCTGACAATCAAGAACGTGGACAAGAAGTTCCAGATGTCTAATATCCTGAGCGCCGTGGTCATGGTGAGCGCCTTCCTGCTGCTGTATGCCCAGGCCCAGAACTGGACCAGCTCCTTTACATTCAATGAGG
AAGTGGGCAGGTACTTTCTGGACCCATCCGGCGATCTGTTCAACAATGGCTACAGATATCTGAACTGGCTGATCGATGTGCCCATGCTGCTGTTTCAGATCCTGTTCGTGGTGTCCCTGACCACATCTAAGTTCT
CTAGCGTGCGGAACCAGTTTTGGTTCTCCGGCGCCATGATGATCATCACCGGCTATATCGGCCAGTTTTACGAGGTGTCTAATCTGACAGCCTTCCTGGTGTGGGGCGCCATCTCCTCTGCCTTCTTTTTCCACA
TCCTGTGGGTCATGAAGAAAGTGATCAACGAGGGCAAGGAGGGAATCTCTCCAGCAGGCCAGAAGATCCTGAGCAACATCTGGATTCTGTTCCTGATCAGCTGGACCCTGTACCCCGGCGCCTATCTGATGCC
TTACCTGACAGGCGTGGACGGCTTCCTGTACTCCGAGGATGGCGTGATGGCAAGGCAGCTGGTGTATACCATCGCCGACGTGAGCTCCAAAGTGATCTACGGCGTGCTGCTGGGCAATCTGGCAATCACCCT
GTCAAAAAACAAGGAACTGGTGGAGGCAAATAGCAAGAGCAGGATCACCAGCGAGGGCGAGTACATCCCCCTGGACCAGATCGACATCAACGTGGTGAGCAAGGGCGAGGAGCTGTTCACCGGGGTGGTG
CCCATCCTGGTCGAGCTGGACGGCGACGTAAACGGCCACAAGTTCAGCGTGTCCGGCGAGGGCGAGGGCGATGCCACCTACGGCAAGCTGACCCTGAAGTTCATCTGCACCACCGGCAAGCTGCCCGTGCCC
TGGCCCACCCTCGTGACCACCTTCGGCTACGGCCTGCAGTGCTTCGCCCGCTACCCCGACCACATGAAGCAGCACGACTTCTTCAAGTCCGCCATGCCCGAAGGCTACGTCCAGGAGCGCACCATCTTCTTCAA
GGACGACGGCAACTACAAGACCCGCGCCGAGGTGAAGTTCGAGGGCGACACCCTGGTGAACCGCATCGAGCTGAAGGGCATCGACTTCAAGGAGGACGGCAACATCCTGGGGCACAAGCTGGAGTACAAC
TACAACAGCCACAACGTCTATATCATGGCCGACAAGCAGAAGAACGGCATCAAGGTGAACTTCAAGATCCGCCACAACATCGAGGACGGCAGCGTGCAGCTCGCCGACCACTACCAGCAGAACACCCCCATC
GGCGACGGCCCCGTGCTGCTGCCCGACAACCACTACCTGAGCTACCAGTCCGCCCTGAGCAAAGACCCCAACGAGAAGCGCGATCACATGGTCCTGCTGGAGTTCGTGACCGCCGCCGGGATCACTCTCGGC
ATGGACGAGCTGTACAAGTTCTGCTACGAGAACGAGGTGTGA

eKR2 = C2C1-KR2-TS-eYFP-ER (ND7/23-cells):

ATGGACTATGGGGGAGCACTGTCCGCCGTCGGGCTGTTTCAGACTTCCTACACCCTGGAGAACAACGGGAGCGTCATTTGCATTCCTAACAATGGCCAGTGCTTCTGTCTGGCCTGGCTGAAGAGCAACGGGA
CCCAGGAACTGGGCAATGCCAACTTTGAGAATTTCATCGGCGCCACCGAGGGCTTTAGCGAGATCGCCTATCAGTTCACCTCCCACATCCTGACACTGGGCTATGCCGTGATGCTGGCCGGCCTGCTGTACTTT
ATCCTGACAATCAAGAACGTGGACAAGAAGTTCCAGATGTCTAATATCCTGAGCGCCGTGGTCATGGTGAGCGCCTTCCTGCTGCTGTATGCCCAGGCCCAGAACTGGACCAGCTCCTTTACATTCAATGAGG
AAGTGGGCAGGTACTTTCTGGACCCATCCGGCGATCTGTTCAACAATGGCTACAGATATCTGAACTGGCTGATCGATGTGCCCATGCTGCTGTTTCAGATCCTGTTCGTGGTGTCCCTGACCACATCTAAGTTCT
CTAGCGTGCGGAACCAGTTTTGGTTCTCCGGCGCCATGATGATCATCACCGGCTATATCGGCCAGTTTTACGAGGTGTCTAATCTGACAGCCTTCCTGGTGTGGGGCGCCATCTCCTCTGCCTTCTTTTTCCACA
TCCTGTGGGTCATGAAGAAAGTGATCAACGAGGGCAAGGAGGGAATCTCTCCAGCAGGCCAGAAGATCCTGAGCAACATCTGGATTCTGTTCCTGATCAGCTGGACCCTGTACCCCGGCGCCTATCTGATGCC
TTACCTGACAGGCGTGGACGGCTTCCTGTACTCCGAGGATGGCGTGATGGCAAGGCAGCTGGTGTATACCATCGCCGACGTGAGCTCCAAAGTGATCTACGGCGTGCTGCTGGGCAATCTGGCAATCACCCT
GTCAAAAAACAAGGAACTGGTGGAGGCAAATAGCGCAGCACCGGTAAAGAGCAGGATCACCAGCGAGGGCGAGTACATCCCCCTGGACCAGATCGACATCAACGTGGTGAGCAAGGGCGAGGAGCTGTTC
ACCGGGGTGGTGCCCATCCTGGTCGAGCTGGACGGCGACGTAAACGGCCACAAGTTCAGCGTGTCCGGCGAGGGCGAGGGCGATGCCACCTACGGCAAGCTGACCCTGAAGTTCATCTGCACCACCGGCAA
GCTGCCCGTGCCCTGGCCCACCCTCGTGACCACCTTCGGCTACGGCCTGCAGTGCTTCGCCCGCTACCCCGACCACATGAAGCAGCACGACTTCTTCAAGTCCGCCATGCCCGAAGGCTACGTCCAGGAGCGCA
CCATCTTCTTCAAGGACGACGGCAACTACAAGACCCGCGCCGAGGTGAAGTTCGAGGGCGACACCCTGGTGAACCGCATCGAGCTGAAGGGCATCGACTTCAAGGAGGACGGCAACATCCTGGGGCACAAG
CTGGAGTACAACTACAACAGCCACAACGTCTATATCATGGCCGACAAGCAGAAGAACGGCATCAAGGTGAACTTCAAGATCCGCCACAACATCGAGGACGGCAGCGTGCAGCTCGCCGACCACTACCAGCAG
AACACCCCCATCGGCGACGGCCCCGTGCTGCTGCCCGACAACCACTACCTGAGCTACCAGTCCGCCCTGAGCAAAGACCCCAACGAGAAGCGCGATCACATGGTCCTGCTGGAGTTCGTGACCGCCGCCGGG
ATCACTCTCGGCATGGACGAGCTGTACAAGTTCTGCTACGAGAACGAGGTGTGA

KR2-TEV-6xHis (*E.coli*):

ATGACGCAGGAACTGGGCAACGCCAACTTTGAAAACTTTATCGGTGCAACGGAAGGCTTTAGCGAAATCGCATACCAATTCACGAGCCATATCCTGACCCTGGGCTACGCAGTTATGCTGGCTGGTCTGCTGT
ATTTCATTCTGACGATCAAAAACGTCGATAAAAAATTCCAGATGAGCAACATCCTGTCTGCAGTGGTTATGGTTTCTGCTTTCCTGCTGCTGTACGCGCAGGCCCAAAACTGGACCAGCTCTTTCACGTTTAATG
AAGAAGTGGGCCGTTATTTCCTGGATCCGAGCGGCGACCTGTTTAACAATGGTTATCGCTACCTGAACTGGCTGATCGACGTTCCGATGCTGCTGTTCCAGATTCTGTTTGTCGTGAGTCTGACCACGTCCAAA
TTTAGTTCCGTGCGTAACCAGTTCTGGTTTAGCGGCGCAATGATGATTATCACCGGCTACATTGGTCAATTCTATGAAGTCTCTAATCTGACGGCTTTTCTGGTGTGGGGTGCGATCTCATCGGCCTTTTTCTTTC
ACATTCTGTGGGTTATGAAGAAAGTGATTAACGAAGGCAAAGAAGGTATCTCACCGGCGGGTCAGAAAATTCTGTCGAATATTTGGATCCTGTTCCTGATCAGTTGGACCCTGTATCCGGGCGCCTACCTGAT
GCCGTATCTGACCGGCGTGGATGGTTTTCTGTATAGTGAAGACGGTGTGATGGCGCGCCAACTGGTTTACACCATCGCCGATGTGAGCTCCAAAGTTATTTATGGCGTCCTGCTGGGTAATCTGGCGATTACCC
TGAGCAAAAACAAAGAACTGGTGGAAGCGAACAGCGAAAATCTGTACTTCCAAGGTCTCGAGCACCACCACCACCACCACTGA

Supplementary Figure 4:

Composition of all buffers used for oocytes and ND7/23-cells

extracellular buffer oocytes	composition [mM]	pH (adjusted with)
Na 10.0	NaCl [100], $MgCl_2$ [1.0], $CaCl_2$ [0.1], glycine [5]	10.0 (NaOH)
Na 7.5	NaCl [100], $MgCl_2$ [1.0], $CaCl_2$ [0.1], MOPS [5]	7.5 (NaOH)
Na 5.0	NaCl [100], $MgCl_2$ [1.0], $CaCl_2$ [0.1], citric acid/Na-citrate [5]	5.0 (NaOH)
KCl 10.0	KCl [100], $MgCl_2$ [1.0], $CaCl_2$ [0.1], glycine [5]	10.0 (KOH)
KCl 7.5	KCl [100], $MgCl_2$ [1.0], $CaCl_2$ [0.1], MOPS [5]	7.5 (KOH)
KCl 5.0	KCl [100], $MgCl_2$ [1.0], $CaCl_2$ [0.1], citric acid [5]	5.0 (KOH)
LiCl 10.0	LiCl [100], $MgCl_2$ [1.0], $CaCl_2$ [0.1], glycine [5]	10.0 (LiOH)
LiCl 7.5	LiCl [100], $MgCl_2$ [1.0], $CaCl_2$ [0.1], MOPS [5]	7.5 (LiOH)
LiCl 5.0	LiCl [100], $MgCl_2$ [1.0], $CaCl_2$ [0.1], citric acid [5]	5.0 (LiOH)
50/50 NaCl/KCl	NaCl [50], KCl [50], $MgCl_2$ [1.0], $CaCl_2$ [0.1], glycine [5]	10.0 (NaOH)
50 KCl	KCl [50], $MgCl_2$ [1.0], $CaCl_2$ [0.1], glycine [5]	10.0 (KOH)
KCl 10.0 (titration)	KCl [200/100/50/25/10/0], glucose [0/0/50/75/90/100], $MgCl_2$ [1.0], $CaCl_2$ [0.1], glycine [5]	10.0 (KOH)
NMG 10.0	NMG [100], $MgCl_2$ [1.0], $CaCl_2$ [0.1], glycine [5]	10.0 (HCl)
NMG 7.5	NMG [100], $MgCl_2$ [1.0], $CaCl_2$ [0.1], MOPS [5]	7.5 (HCl)
Na-Gluk 10.0	Na-gluconate [100], $MgCl_2$ [1.0], $CaCl_2$ [0.1], glycine [5]	10.0 (NaOH)
Na-Gluk 7.5	Na-gluconate [100], $MgCl_2$ [1.0], $CaCl_2$ [0.1], MOPS [5]	7.5 (NaOH)
$MgCl_2$ 7.5	$MgCl_2$ [100], $CaCl_2$ [0.1], MOPS [5]	10.0 (NaOH)
$CaCl_2$ 7.5	$MgCl_2$ [1.0], $CaCl_2$ [100], MOPS [5]	7.5 (NaOH)

extracellular buffer ND7/23-cells	composition [mM]	pH (adjusted with)	osmolarity (adjusted with glucose)
NaCl 9.0	NaCl [110], KCl [1], $MgCl_2$ [1.0], $CaCl_2$ [1.0], Tris [10], TEA [20], CsCl [5], $BaCl_2$ [5]	9.0 (HCl)	310 mOsm
KCl 9.0	NaCl [1], KCl [110], $MgCl_2$ [1.0], $CaCl_2$ [1.0], Tris [10], TEA [20], CsCl [5], $BaCl_2$ [5]	9.0 (HCl)	310 mOsm
LiCl 9.0	NaCl [1], KCl [1], LiCl [110], $MgCl_2$ [1.0], $CaCl_2$ [1.0], Tris [10], TEA [20], CsCl [5], $BaCl_2$ [5]	9.0 (HCl)	310 mOsm

intracellular buffer ND7/23-cells	composition [mM]	pH (adjusted with)	osmolarity (adjusted with glucose)
0.1 mM NaCl 0.1 mM KCl pH 7.2	NaCl [0.1], KCl [0.1], NMG [110], $MgCl_2$ [1.0], $CaCl_2$ [1.0], EGTA [10], HEPES [10]	7.2 (HCl)	290 mOsm
1 mM NaCl 1 mM KCl pH 7.2	NaCl [1], KCl [1], NMG [110], $MgCl_2$ [1.0], $CaCl_2$ [1.0], EGTA [10], HEPES [10]	7.2 (HCl)	290 mOsm
110 mM NaCl 1 mM KCl pH 7.2	NaCl [110], KCl [1], $MgCl_2$ [1.0], $CaCl_2$ [1.0], EGTA [10], HEPES [10]	7.2 (NaOH)	290 mOsm
1 mM NaCl 110 mM KCl pH 7.2	NaCl [1], KCl [110], $MgCl_2$ [1.0], $CaCl_2$ [1.0], EGTA [10], HEPES [10], TEA [20], CsCl [5], $BaCl_2$ [5]	7.2 (KOH)	290 mOsm
1 mM NaCl 1 mM KCl 110 mM LiCl pH 7.2	NaCl [1], KCl [1], LiCl [110], $MgCl_2$ [1.0], $CaCl_2$ [1.0], EGTA [10], HEPES [10]	7.2 (LiOH)	290 mOsm

Supplementary Figure 5

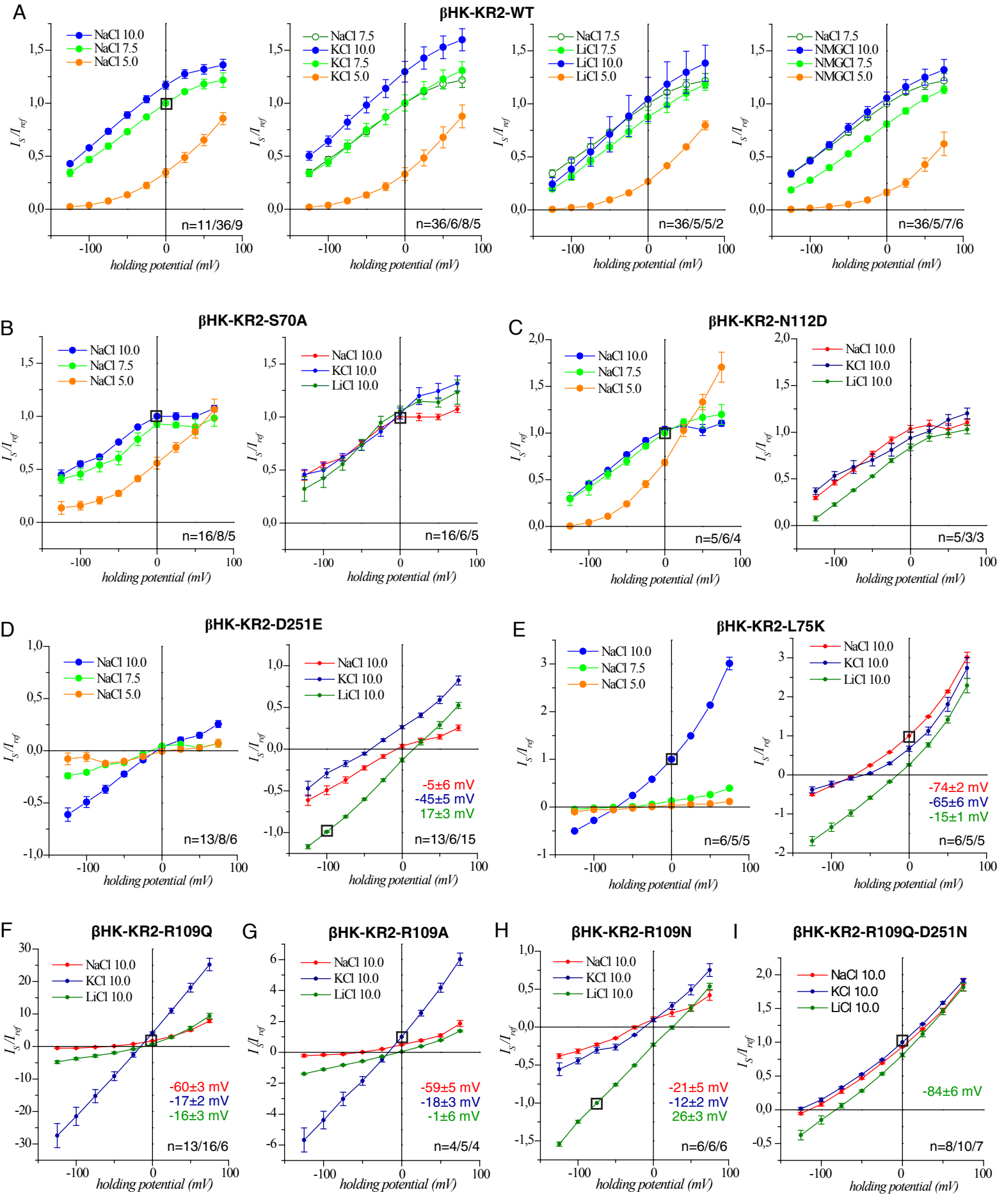

Supplementary Figure 5: Current-voltage plots for various KR2 mutants, measured in *Xenopus laevis* oocytes. Cells were measured at different pH_o values or cation conditions. Reversal potentials are indicated, if possible, and where appropriate. Small black boxes show the respective condition used for normalization.

Supplementary Figure 6

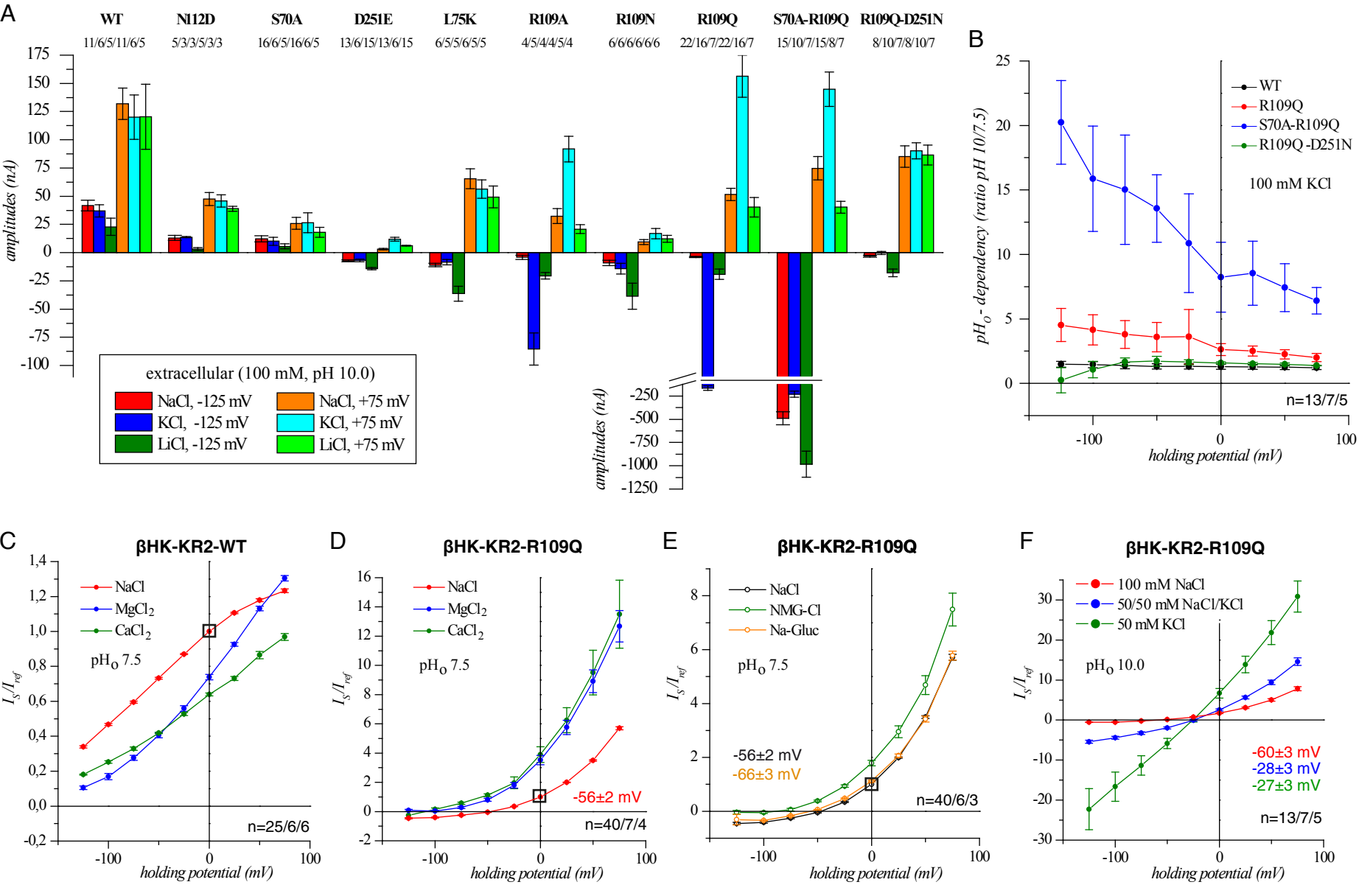

Supplementary Figure 6: Additional results obtained from electrophysiological measurements in oocytes. (*A*) Comparison of the absolute stationary photocurrent amplitudes for different extracellular buffer conditions and holding potentials. The mutants D116N and D251N are not shown because no obvious stationary photocurrents were observed. (*B*) The pH_o-dependency is illustrated as the ratio between the photocurrents at pH_o 10.0 and pH_o 7.5 (with 100 mM KCl). Current-voltage plots for (*C*) KR2-WT and (*D-E*) KR2-R109Q at different extracellular ion conditions (all at a concentration of 100 mM). Ca^{+2} and Mg^{+2} are not transported but influence the photocurrents, whereas removal of extracellular Cl^- does not influence photocurrents. Data indicate minor passive Na^+ conductance. Small black boxes show the respective condition used for normalization. (*F*) Current-voltage-plot of KR2-R109Q in different extracellular Na^+ and K^+ concentrations, illustrating the competition between Na^+ and K^+(photocurrents were normalized to 100 mM NaCl, pH_o 7.5, not shown in this plot). K^+determines the reversal potential, whereas Na^+ shows an inhibitory effect.

Supplementary Figure 7

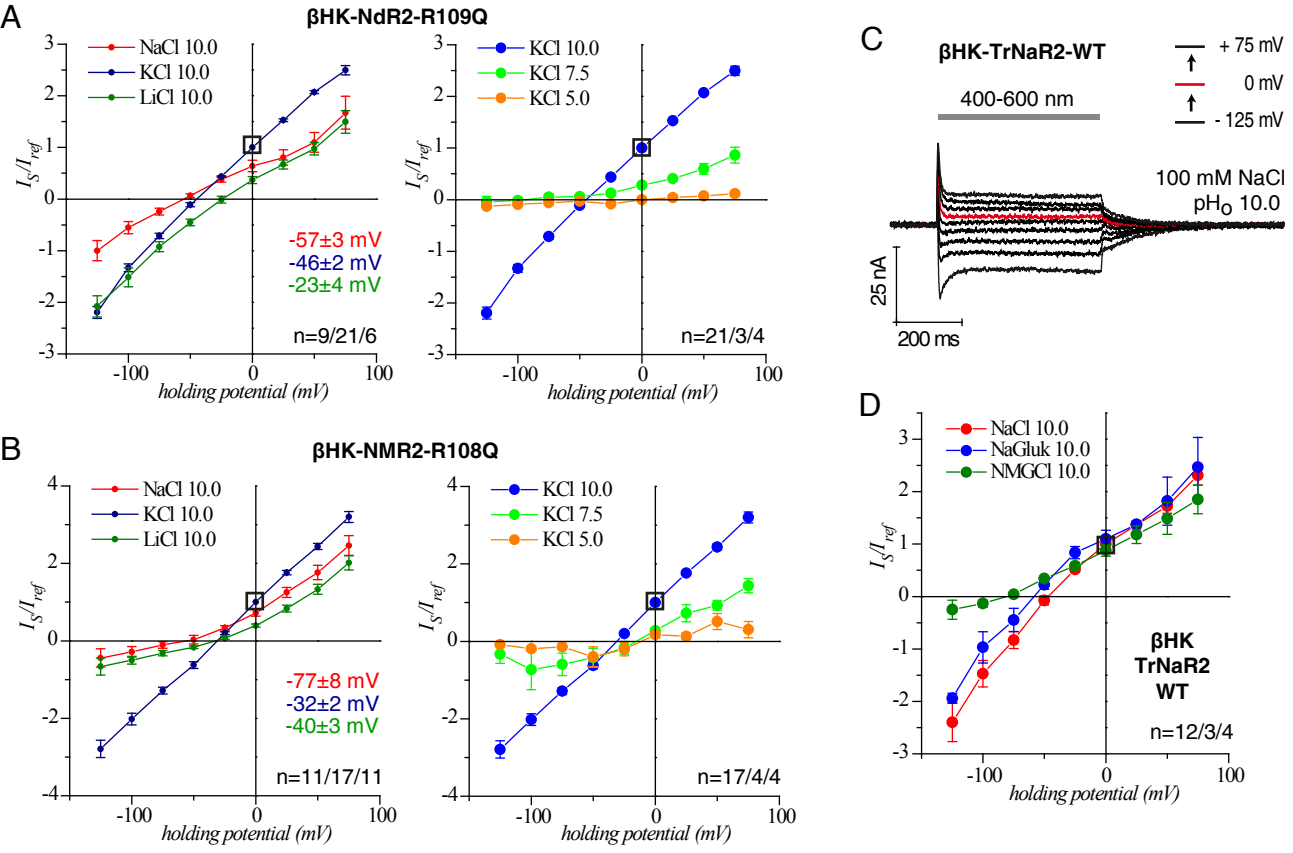

Supplementary Figure 7: Further electrophysiological analysis of NdR2βHK-R109Q, NMR2βHK-R108Q, and TrNaR2βHK-WT in oocytes. (*A-B*) Current-voltage plots of NdR2βHK-R109Q and NMR2βHK-R108Q demonstrate different ion-selectivities of the mutants and their pHo-dependency (normalized to 100 mM KCl, pHo 10, and 0 mV). (*C*) Photocurrent traces of TrNaR2βHK-WT indicate leakiness in the WT protein. However, amplitudes were poor, and only the best measurement is shown. (*D*) Current-voltage plot of TrNaR2βHK-WT after removal of Cl^-or Na^+ ions (normalized to 100 mM NaCl, pHo 10, and 0 mV. Results indicate leakiness for cations.

Supplementary Figure 8

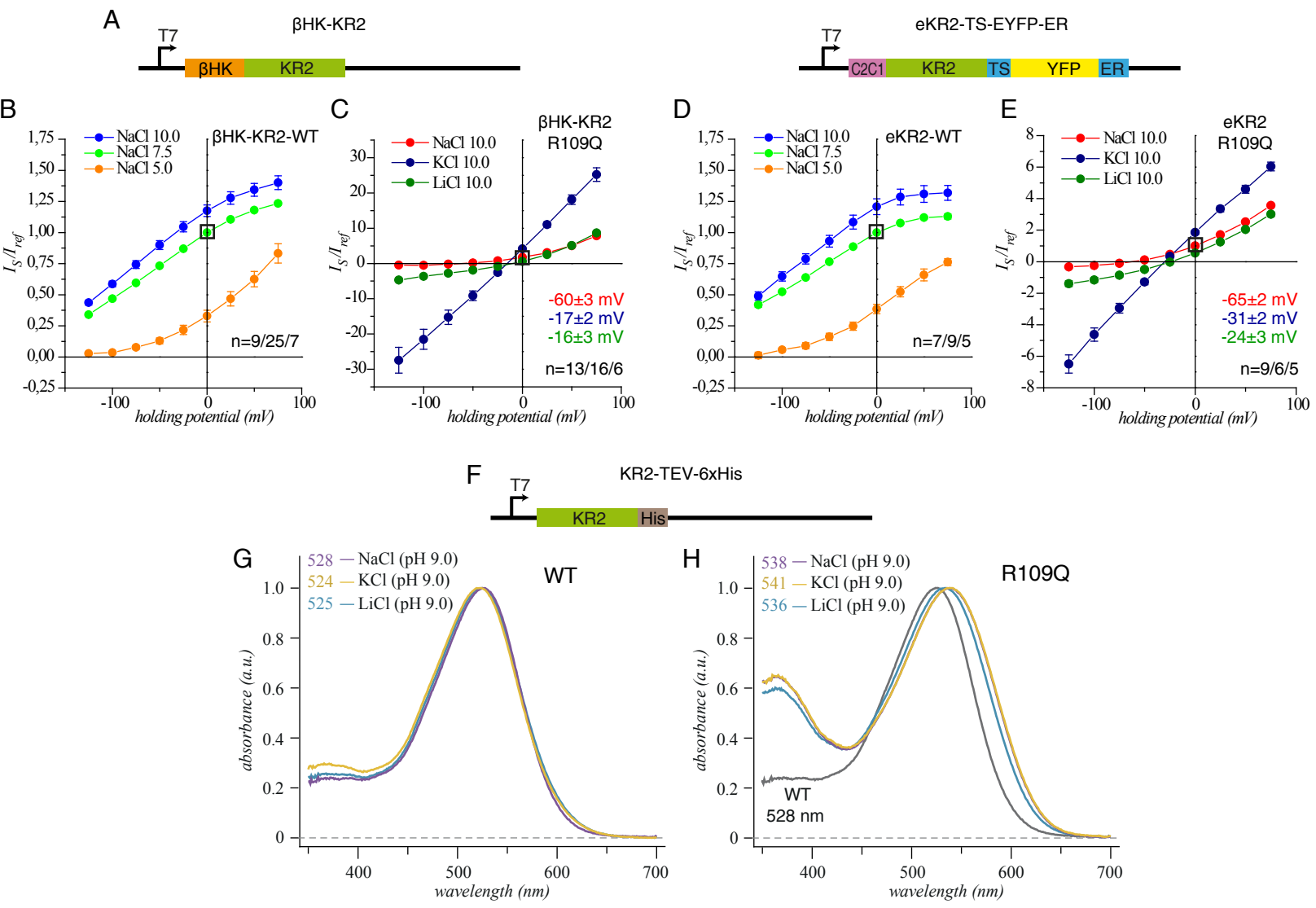

Supplementary Figure 8: Influence of construct design and spectral characteristics of KR2. (*A*) Structure of the targeting constructs KR2βHK and eKR2; nucleotide sequences of each construct are shown in Supplementary Fig. 3. (*B-E*) Comparison of the two targeting constructs, both tested in oocytes, for KR2-WT and KR2-R109Q. Photocurrents were normalized to 0 mV, 100 mM NaCl, and pH 7.5 (WT) or pH 10.0 (R109Q). The pH_o-dependency was similar for all constructs, but differences in the reversal potentials were observed for KR2-R109Q. (*F*) The constructs utilized for the pH-assay and for purification from *E. coli* are functional without any additional targeting. (*G-H*) Absorption spectra of purified KR2-WT and KR2-R109Q, measured at pH 9.0 and in 110 mM of the indicated salt. KR2-R109Q is characterized by an increased amount of protein with a deprotonated Schiff-base (365 nm) and an increased cation-dependency of the absorption maxima.

Supplementary Figure 9

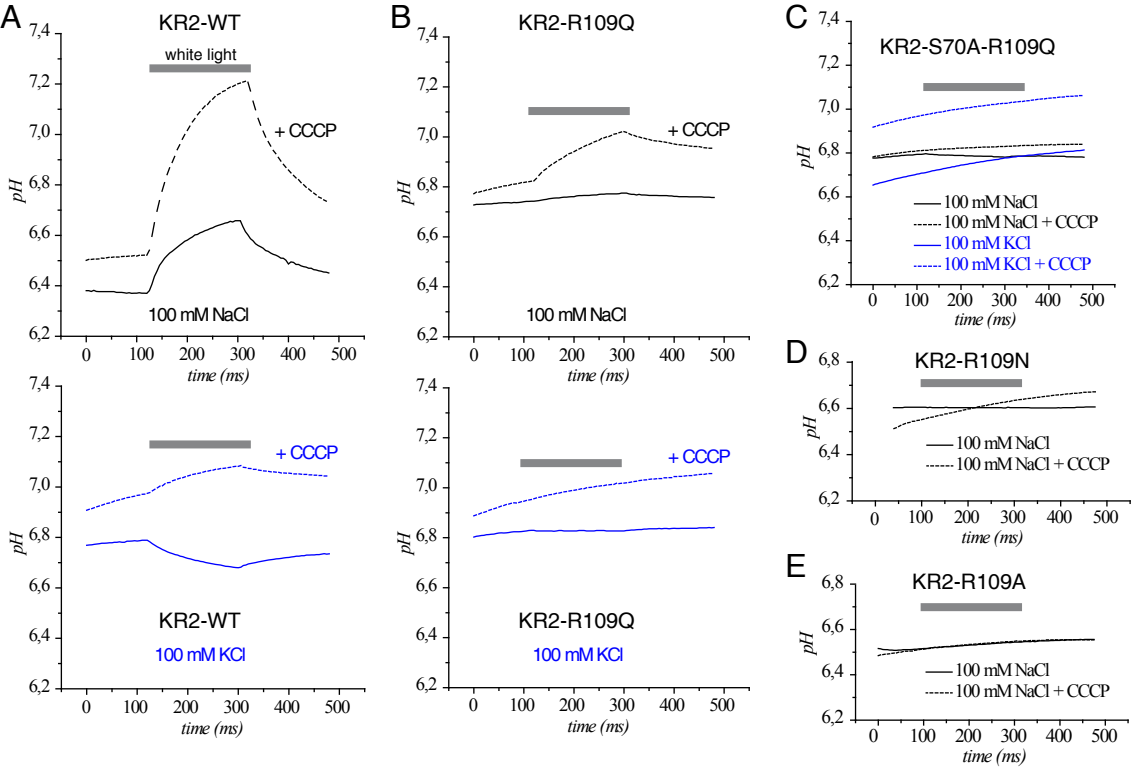

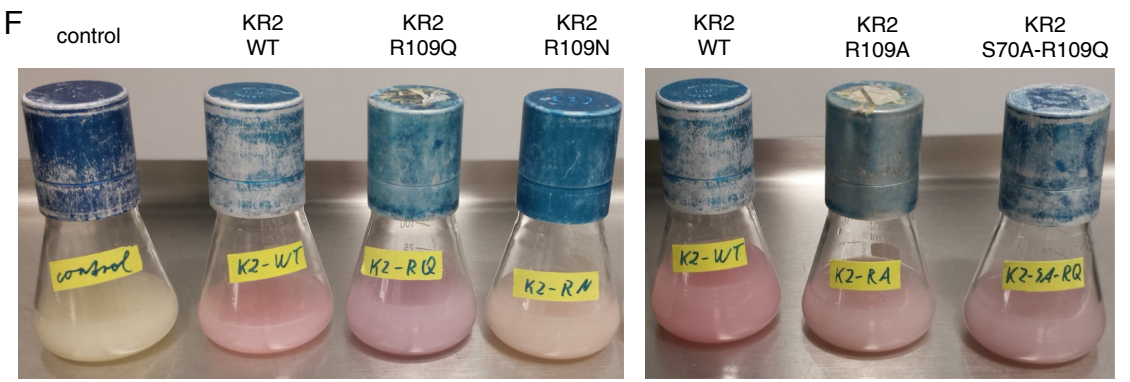

Supplementary Figure 9: Analysis of light-induced pH changes in suspensions of *Escherichia coli* expressing various KR2 mutants. Suspensions of cells expressing (*A*) KR2-WT, (*B, D-E*) KR2-R109Q/N/A, and (*C*) KR2-S70A-R109Q were tested before (continuous line) and after (dotted lines) addition of the protonophore, carbonyl cyanide m-chlorophenyl hydrazone (CCCP). Only WT and R109Q KR2 exhibited pH-changes during illumination. (*F*) Photos *E. coli* cell cultures are shown (all concentrated to OD_{600} =10). The faint colors of KR2-R109N, KR2-R109Q, and KR2-S70A-R109Q indicate lower protein expression.

Supplementary Figure 10:

Overview of all KR2 constructs and mutants tested in oocytes

	location/motivation/earlier investigations in KR2	**results**
KR2-WT	/	only positive currents
βKR2-WT	/	only positive currents
eKR2-WT	/	only positive currents
βKR2-L32E	extracellular half channel, interaction partner of R109	positive currents + negative currents with K and Li at high elechtrochemical load (-125 mV)
βKR2-S60T	ion uptake region	only positive currents
βKR2-N61P	ion uptake region, increased proton pumping proposed by Kato et al. 2015 (N61Y), Gushchin et al. 2015 (N61M)	only positive currents
βKR2-S64T	ion uptake region	only positive currents
βKR2-S70A	counter-ion complex, Kato 2015 et al. (S70T/A)	studied intensively in this study
βKR2-S70V	counter-ion complex, Kato 2015 et al. (S70T/A)	similar to S70A
βKR2-L75K	counter-ion complex, Inoue et al. 2013 (R109A)	studied intensively in this study
βKR2-R109Q	counter-ion complex, Inoue et al. 2013 (R109A)	studied intensively in this study
βKR2-R109A	counter-ion complex, Inoue et al. 2013 (R109A)	studied intensively in this study
βKR2-R109N	counter-ion complex, Inoue et al. 2013 (R109A)	studied intensively in this study
βKR2-N112D	counter-ion complex, Inoue et al. 2013 (N112A/D)	studied intensively in this study
βKR2-D116N	counter-ion complex, Inoue et al. 2013 (D116A/E/N)	studied intensively in this study
βKR2-D116E	counter-ion complex, Inoue et al. 2013 (D116A/E/N)	only positive currents, low amplitudes
βKR2-Q244E	ion-release cavity, interaction partner of R109	only positive currents
βKR2-D251N	counter-ion complex, Inoue et al. 2013 (D251A/E/N)	studied intensively in this study
βKR2-D251E	counter-ion complex, Inoue et al. 2013 (D251A/E/N)	studied intensively in this study
βKR2-G263W	ion uptake region, increased potassium pumping proposed by Kato et al. 2015 (G263W) and Gushchin et al. 2015 (G263F/G263L)	only positive currents
βKR2-N61P-G263W	ion uptake region, increased potassium pumping proposed by Kato et al. 2015	only positive currents, low amplitudes, pronounced transient peak current
βKR2-R109Q-E11D	ion-release cavity, Gushchin et al. 2015 (E11A), Kato et al. 2015 (E11A)	leaky , low amplitudes
βKR2-R109Q-E18Q	extracellular side	leaky , low amplitudes
βKR2-R109Q-F20A	ion-release cavity	leaky , low amplitudes
βKR2-R109Q-E22Q	extracellular side	similar to R109Q

βKR2-R109Q-T33D	transmembrane surface of KR2	very low amplitudes
βKR2-R109Q-V67A	interaction with Schiff-base from intracellular side	leaky for Na/K/Li, high amplitudes (but lower than R109Q-S70A)
βKR2-R109Q-S70A	see single mutations	studied intensively in this study
βKR2-R109Q-S70V	see single mutations	similar to R109Q-S70A but lower amplitudes
βKR2-R109Q-L75K	see single mutations	similar to R109Q
βKR2-R109Q-L75T	see single mutations	leaky for Na/K/Li, low amplitudes
βKR2-R109Q-E91Q	extracellular side	leaky , low amplitudes
βKR2-R109Q-R94Q	extracellular side	leaky , low amplitudes
βKR2-R109Q-D98N	extracellular side	leaky
βKR2-R109Q-D102N	extracellular side, Gushchin et al. 2015 (D102N), Kato et al. 2015 (D102N)	leaky
βKR2-R109Q-N112D	see single mutations	similar to R109Q leaky
βKR2-R109Q-D116N	see single mutations	no stationary currents
βKR2-R109Q-D116E	see single mutations	leaky, very low amplitudes
βKR2-R109Q-D116A	see single mutations	no stationary currents
βKR2-R109Q-L120D	interaction with Schiff-base from intracellular side	no currents
βKR2-R109Q-Q123A	ion uptake region, Inoue et al. 2013 (Q123A/E/D)	leaky, low amplitudes
βKR2-R109Q-E160Q	ion-release cavity, Inoue et al. (E160Q), Gushchin et al. 2015 (E160A), Kato et al. 2015 (E160A)	leaky
βKR2-R109Q-E237Q	extracellular side	leaky
βKR2-R109Q-R243Q	ion-release cavity, Gushchin et al. 2015 (R243Q/A), Kato et al. 2015 (R243A)	leaky, low amplitudes
βKR2-R109Q-D251N	see single mutations	studied intensively in this study
βKR2-R109Q-D251E	see single mutations	leaky for Na/K/Li, low amplitudes, pH_o-dependency further increased
βKR2-R109Q-D251T	see single mutations	very low amplitudes
βKR2-R109Q-D251H	see single mutations	very low amplitudes
ßKR2-R109Q-S254D	interaction with Schiff-base from intracellular side	no currents
βKR2-R109Q-S70A-L75K	see single mutations	leakyness for Na/K/Li, very high amplitudes for Li
βKR2-R109Q-N112D-D251N	see single mutations	no stationary currents
βKR2-R109Q-N61P-G263W	see single mutations	no currents
eKR2-R109A	see single mutations	studied intensively in this study
eKR2-R109Q	see single mutations	studied intensively in this study
eKR2-R109Q-S70A	see single mutations	studied intensively in this study